

Letters

Magnetic domains in Co_{17}R_2 , $(\text{Co,Fe})_{17}\text{R}_2$, and Co_7R_2 compounds

The excellent permanent magnet properties of Co_5R^* compounds [1-3] are based on a high, positive, uniaxial magnetocrystalline anisotropy. This "easy-axis" magnetic symmetry produces magnetic domain patterns [4-8] of a type well characterized by earlier work on other easy-axis materials [9-12].

The Co-R alloy system contains Co_{17}R_2 and Co_7R_2 phases with crystal structures closely related to that of the Co_5R compounds [13]. The Co_7R_2 phases, of potential interest as permanent magnet materials, are generally of easy-plane, rather than easy-axis, magnetic symmetry. However, Ray and Strnat [14] have recently reported that partial substitution of iron for cobalt in some cases transforms the symmetry to easy-axis. The Co_7R_2 phases are not of direct

interest as permanent magnet materials, but are of indirect interest because optimum Co_5R magnets are hyperstoichiometric and contain several per cent of Co_7R_2 [3, 15].

We have studied magnetic symmetries in several Co_{17}R_2 , $(\text{Co, Fe})_{17}\text{R}_2$, and Co_7R_2 phases by means of magnetic domain observations.

Compounds were arc-cast from high-purity materials and studied metallographically either in the as-cast condition or after annealing 16 to 20 h 100 to 200°C below their respective melting points. Domains were observed in polarized light on a Bausch and Lomb metallograph, using an elliptical compensator [16] to optimize the contrast.

As shown earlier by Becker [1], an as-cast sample of $\text{Co}_{17}\text{Sm}_2$ contains classic easy-axis domain structures (Fig. 1). Magnetic domain walls in such materials lie nearly parallel to the magnetization direction. Therefore, in grains in which this easy-axis has a substantial component in the surface plane, the domain patterns are elongated in this direction. However, in grains with the easy-axis nearly normal to the surface, "rosette" patterns are seen, as in the grain at the top in Fig. 1. These patterns result from a surface refinement of the domain structure that occurs to reduce magnetostatic energy [6, 9-12]. Domain walls become corrugated in the surface region, domains are split by reverse "spike" domains, and the resulting rosette patterns are sufficiently characteristic that their observation can be taken as evidence of easy-axis magnetic symmetry. For example, Fig. 2a shows domains in a casting of composition $(\text{Co}_{0.75}\text{Fe}_{0.25})_{17}\text{Sm}_2$. This confirms results of Ray and Strnat [14] that easy-axis symmetry is retained in this system.

In contrast, we were unable to detect any magnetic domain structures in as-cast or annealed samples of $\text{Co}_{17}\text{Pr}_2$, Co_{17}Y_2 , or $\text{Co}_{17}\text{Nd}_2$. An as-cast sample of $\text{Co}_{17}\text{Ce}_2$ contained two phases and faint lamellar domains, but an annealed sample was single phase and showed no domains. These results are consistent with earlier results that these four compounds have easy-plane rather than easy-axis symmetry [1, 2, 14]. Presumably the magnetization in each domain can rotate freely in the easy plane and, to decrease magnetostatic energy, will lie parallel to the surface. The Kerr-effect contrast in Co-R

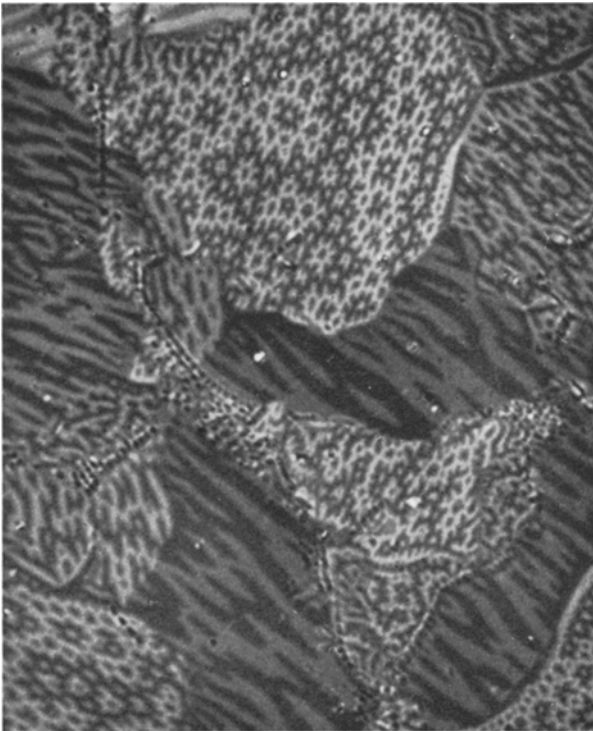


Figure 1 Magnetic domains in $\text{Co}_{17}\text{Sm}_2$. Rosette structure in grain at top is characteristic of easy-axis magnetic symmetry (photograph from J. J. Becker) ($\times 400$).

*R = rare earth, La, or Y.

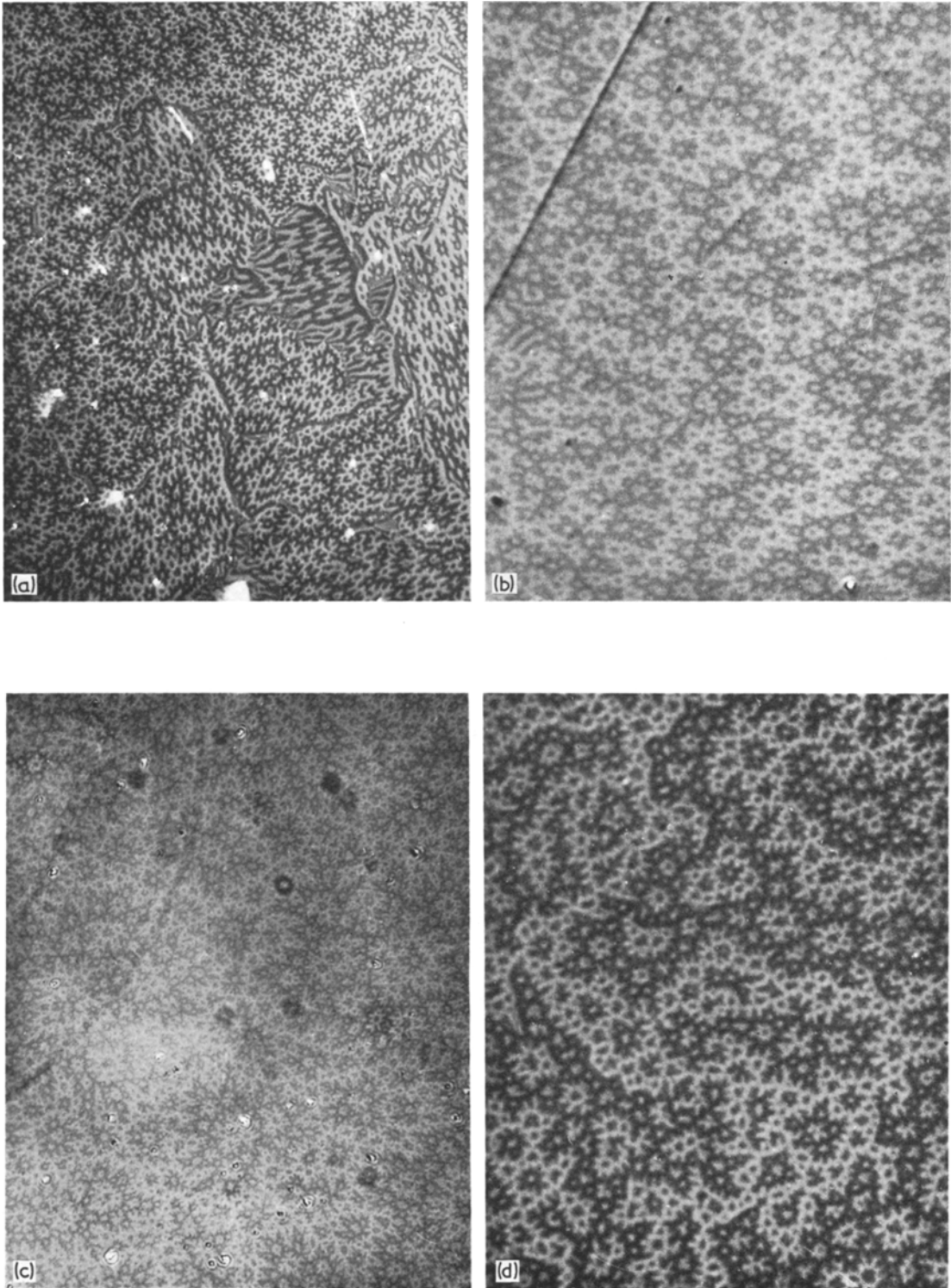


Figure 2 Easy-axis domain patterns in (a) $(\text{Co}_{0.75}\text{Fe}_{0.25})_{17}\text{Sm}_2$; (b) $(\text{Co}_{0.6}\text{Fe}_{0.4})_{17}\text{Pr}_2$; (c) $(\text{Co}_{0.7}\text{Fe}_{0.3})_{17}\text{Y}_2$; (d) $(\text{Co}_{0.7}\text{Fe}_{0.3})_{17}\text{Gd}_2$ ($\times 550$).

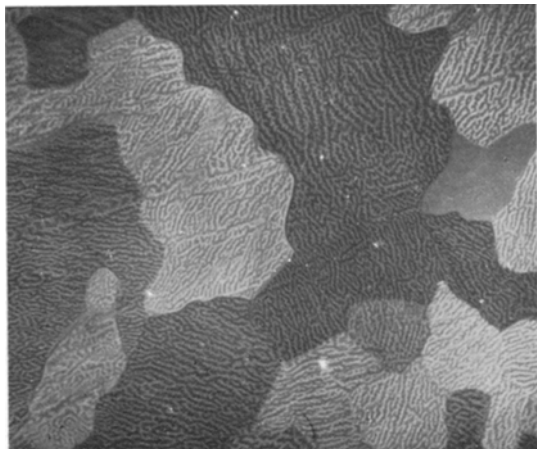


Figure 3 Domain patterns in mechanically polished $\text{Co}_{17}\text{Gd}_2$. These maze patterns are believed to be caused by surface strains ($\times 400$).

compounds arises primarily from the component of magnetization normal to the surface, and thus domains are not seen in these easy-plane materials. Substitution of iron for cobalt in $\text{Co}_{17}\text{Pr}_2$, Co_{17}Y_2 , and $\text{Co}_{17}\text{Ce}_2$ transforms the magnetic symmetry to easy-axis [14], as con-

firmed by the domain patterns in Figs. 2b and c and equivalent patterns seen in $(\text{Co}_{0.75}\text{Fe}_{0.25})_{17}\text{Ce}_2$.

Mechanically polished surfaces of $\text{Co}_{17}\text{Gd}_2$ reveal a fine and complex domain structure (Fig. 3). This structure appears to be related to surface strain introduced by polishing, an effect well known in soft magnetic materials [17]. If a strain-free surface is prepared by electropolishing in phosphoric acid, a fine but very faint rosette domain pattern can be seen. (On $\text{Co}_{17}\text{Sm}_2$ and other compounds tested, domains on mechanically polished and electropolished surfaces appeared the same.) We conclude that $\text{Co}_{17}\text{Gd}_2$ is of easy-axis symmetry, but probably has a rather low crystal anisotropy. If 30% of the cobalt is replaced by iron, coarser easy-axis patterns of much stronger contrast are seen (Fig. 2d).

Prior to this work, no information was available on the magnetic symmetry of Co_7R_2 compounds. We have observed easy-axis patterns in annealed samples of Co_7Sm_2 (Fig. 4a), Co_7Pr_2 (Fig. 4b), Co_7Y_2 , Co_7Nd_2 , and Co_7La_2 . Patterns were also easy-axis in as-cast samples, but were more complex because grain structure was fine and complex.

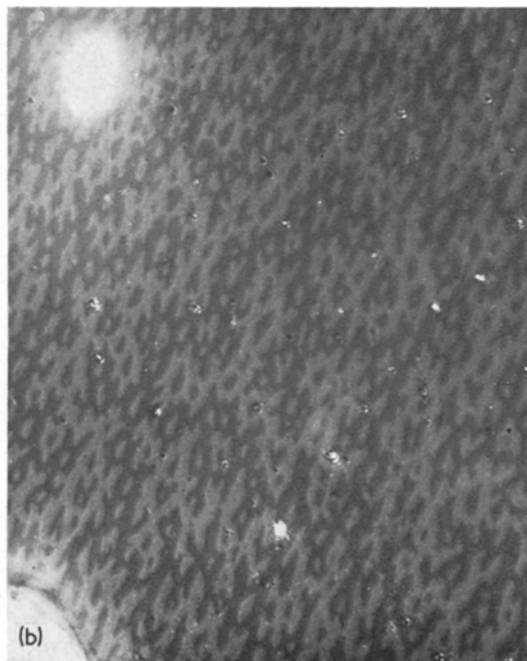
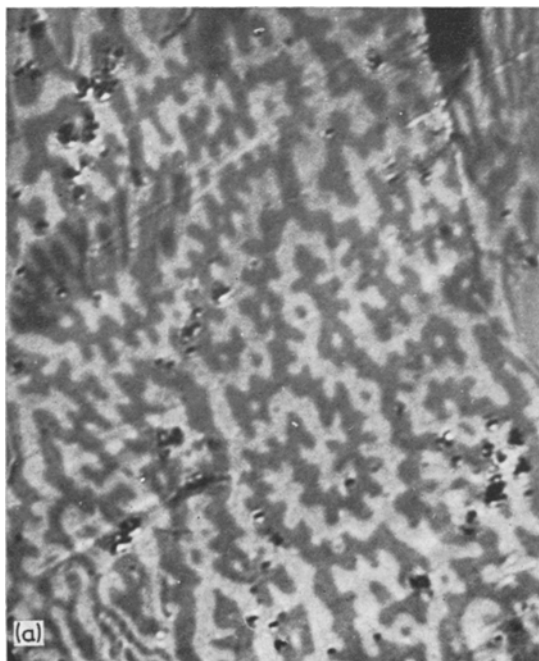


Figure 4 Easy-axis domain patterns in (a) Co_7Sm_2 , (b) Co_7Pr_2 ($\times 550$).

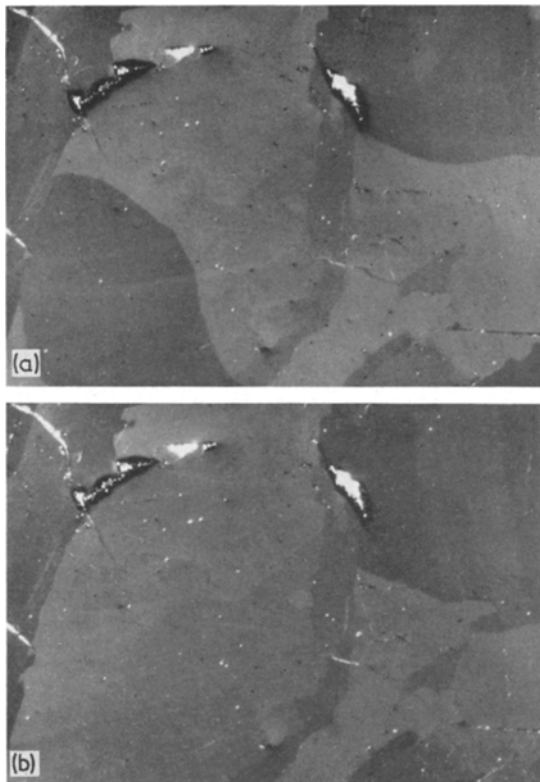


Figure 5 Magnetic domains in Co_7Gd_2 (a) before and (b) after touching sample with a magnet. Note downward motion of domain wall at right centre and disappearance of dark domain at lower left. Domains are large because of low magnetic moment ($\times 250$).

An interesting special case is Co_7Gd_2 . Because the Gd and Co moments are antiparallel, this compound has a very low net moment [18], which leads us to expect very large domains [9-12]. The domain size was in fact found to be comparable to the grain size, and domains were most easily recognized by comparing the same area before and after moving the domains with a magnet (Fig. 5). Our observations on this sample were consistent with earlier observations on easy-axis materials with low moment [9-12].

In summary, characteristic easy-axis domain patterns were seen in $\text{Co}_{17}\text{Sm}_2$, $\text{Co}_{17}\text{Gd}_2$, and several $(\text{Co}, \text{Fe})_{17}\text{R}_2$ and Co_7R_2 compounds. Domains were not seen in $\text{Co}_{17}\text{Pr}_2$, Co_{17}Y_2 , $\text{Co}_{17}\text{Nd}_2$, or $\text{Co}_{17}\text{Ce}_2$.

In a recent study of domain widths and domain-wall energies in Co_5R compounds [19], it was suggested that the wavelength of surface domain corrugations on bulk samples may be

a rough measure of the fineness of grain size necessary to produce good coercive forces in sintered magnets. For example, this dimension was about $6\ \mu\text{m}$ in Co_5Sm , $3\ \mu\text{m}$ in Co_5Pr , and $30\ \mu\text{m}$ in Co_5Gd . Applying this criterion to the domain patterns reported above, we estimate this dimension to be 1 to $2\ \mu\text{m}$ in $\text{Co}_{17}\text{Gd}_2$ and the various $(\text{Co}, \text{Fe})_{17}\text{R}_2$ compounds, 2 to $3\ \mu\text{m}$ for $\text{Co}_{17}\text{Sm}_2$ and most of the Co_7R_2 compounds, $5\ \mu\text{m}$ for Co_7Sm_2 , and very large but undetermined for Co_7Gd_2 . In combination with saturation magnetization values, these dimensions may also be used to estimate domain-wall energies [19].

Acknowledgements

We are grateful to J. J. Becker for allowing us to use Fig. 1 and for providing many of the samples. Metallography was done by M. B. McConnell, D. Marsh, and A. Ritzer. This work was supported by the Advanced Research Projects Agency, Department of Defense, and was monitored by the Air Force Materials Laboratory, MAYE, under Contract F33615-70-C-1626.

References

1. J. J. BECKER, *J. Appl. Phys.* **41** (1970) 1055.
2. K. J. STRNAT and A. E. RAY, *Z. Metallk.* **61** (1970) 461.
3. D. L. MARTIN and M. G. BENZ, Proc. 1971 Conf. on Magnetism and Magnetic Materials, Amer. Inst. Physics Conf. Proc. No. 5 (1972) 970.
4. E. A. NESBITT, H. J. WILLIAMS, J. H. WERNICK, and R. C. SHERWOOD, *J. Appl. Phys.* **33** (1962) 1674.
5. R. A. MCCURRIE and G. P. CARSWELL, *J. Mater. Sci.* **5** (1970) 825; R. A. MCCURRIE, G. P. CARSWELL, and J. B. O'NEILL, *ibid* **6** (1971) 164.
6. K. BACHMANN, A. BISCHOFBERGER, and F. HOFER, *ibid* **6** (1971) 169; K. BACHMANN and F. HOFER, *Z. Angew. Physik* **32** (1971) 41; K. BACHMANN, *IEEE Trans. Mag.* **7** (1971) 647.
7. R. G. WELLS and D. V. RATNAM, *IEEE Trans. Mag.* **7** (1971) 651.
8. F. F. WESTENDORP, *J. Appl. Phys.* **42** (1971) 5727.
9. J. KACZER, *IEEE Trans. Mag.* **6** (1970) 442; *Sov. Phys. -JETP* **19** (1964) 1204.
10. M. ROSENBERG, C. TANASOIU, and V. FLORESCU, *J. Appl. Phys.* **37** (1966) 3826.
11. A. HUBERT, *Phys. Stat. Sol.* **24** (1967) 669.
12. D. J. CRAIK, *Contemp. Phys.* **11** (1970) 65; D. J. CRAIK and R. S. TEBBLE, "Ferromagnetism and Ferromagnetic Domains" (Wiley and Sons, New York, 1965).
13. K. H. J. BUSCHOW, *Phys. Stat. Sol. (a)* **7** (1971) 199; *Philips Res. Repts.* **26** (1971) 49.

14. A. E. RAY and K. J. STRNAT, 1972 Intermag Conf., Kyoto, to be published in *IEEE Trans. Mag.* **8** (1972).
15. R. E. CECH, *J. Appl. Phys.* **41** (1970) 5247; D. K. DAS, *IEEE Trans. Mag.* **7** (1971) 432.
16. A. F. TURNER, J. R. BENFORD, and W. J. MCLEAN, *Economic Geology* **40** (1945) 18.
17. S. CHIKAZUMI and K. SUZUKI, *J. Phys. Soc. Japan* **10** (1955) 523.
18. R. LEMAIRE, *Cobalt* **33** (1966) 201.
19. J. D. LIVINGSTON, *J. Appl. Phys.* to be published.

Received 15 May and
accepted 17 July 1972

J. D. LIVINGSTON
General Electric Corporate
Research and Development
Schenectady, New York, USA

Orthorhombic diglycine sulphate

We note with interest the recent publication on the growth and properties of monoclinic diglycine sulphate monohydrate [1]. Crystals grown under similar conditions and studied here have proved to be anhydrous diglycine sulphate with an orthorhombic structure, almost certainly the same orthorhombic diglycine sulphate mentioned by Wood and Holden [2]. Large clear crystals could be grown at 30°C from water solutions of glycine and sulphuric acid in 1:1 proportions; the crystals are tabular in habit (Fig. 1) and exhibit perfect cleavage parallel to the {010}

(NH₂CH₂COOH)₂.H₂SO₄ is 39.52%. The nitrogen content, 11.5% by wt, gives a calculated nitrogen:sulphur atomic ratio of 2.04:1, confirming that the new material is diglycine sulphate. Its measured density (ρ_m) was 1.743, which compares well with the calculated density (ρ_x) ($Z = 8$) of 1.72 from the X-ray data for (NH₂CH₂COOH)₂.H₂SO₄.

Futher studies revealed that, unlike the other two glycine sulphates, anhydrous diglycine sulphate does not show any crystallographic transition between room temperature and its decomposition temperature. Differential thermal analysis indicates decomposition of the compound at temperatures above 150°C.

Dielectric measurements on plates cleaved or cut perpendicular to the crystallographic axes gave dielectric constants of 7.5, 7.0 and 14.5 in

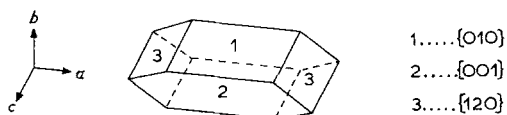


Figure 1 Diglycine sulphate; crystal habit.

face. Proportions of amino acid to sulphuric acid of 2:1 and 3:1 always gave triglycine sulphate (TGS). X-ray powder photographs (Table I) demonstrated that the crystals grown from 1:1 solution differed from TGS.

X-ray examination of the new crystals by Weissenberg techniques showed that they belong to the orthorhombic class, with parameters:

$$a_0 = 10.93\text{\AA} \quad b_0 = 17.74\text{\AA} \quad c_0 = 9.88\text{\AA}$$

Table II compares this material with the other two glycine sulphates that have been described in the literature.

A Gieber-Scheiber test (for piezoelectricity) in powdered samples of the new compound proved negative, suggesting a crystallographic point group of *mmm*.

Chemical analysis of these crystals showed a sulphuric acid content of 39.5% by wt; the calculated sulphuric acid content for

TABLE I Powder data for diglycine sulphate

Intensity	d_{obs}
m	9.0
w	6.9
m	5.6
vw	5.45
vw	4.95
s	4.78
s	4.68
m	4.45
ms	4.35
s	3.8
mw	3.73
mw	3.68
s	3.6
s	3.38
s	3.2
vs	2.97
w	2.81
m	2.78
m	2.52
m	2.48
m	2.39